




Nuclear charge radii of Na isotopes: Interplay of atomic and nuclear theoryB. Ohayon ^{1,*}, R. F. Garcia Ruiz,² Z. H. Sun ^{3,4}, G. Hagen,^{3,4} T. Papenbrock ^{4,3} and B. K. Sahoo ^{5,†}¹*Institute for Particle Physics and Astrophysics, ETH Zürich, CH-8093 Zürich, Switzerland*²*Massachusetts Institute of Technology, Cambridge, Massachusetts 02139, USA*³*Physics Division, Oak Ridge National Laboratory, Oak Ridge, Tennessee 37831, USA*⁴*Department of Physics and Astronomy, University of Tennessee, Knoxville, Tennessee 37996, USA*⁵*Atomic, Molecular and Optical Physics Division, Physical Research Laboratory, Navrangpura, Ahmedabad 380058, Gujarat, India*

(Received 26 September 2021; revised 23 November 2021; accepted 11 March 2022; published 28 March 2022)

The accuracy of atomic theory calculations limits the extraction of nuclear charge radii from isotope shift measurements of odd-proton nuclei. For Na isotopes, though precise spectroscopic measurements have existed for more than half a century, calculations by different methods offer a wide range of values. Here, we present accurate atomic calculations to reliably extract the Na charge radii. By combining experimental matter radii with nuclear coupled-cluster calculations based on nucleon-nucleon and three-nucleon forces, we constrain the parameters obtained from the atomic calculations. Therefore, this study guides atomic theory and highlights the importance of using accurate atomic and nuclear computations in our understanding of the size of light nuclei.

DOI: [10.1103/PhysRevC.105.L031305](https://doi.org/10.1103/PhysRevC.105.L031305)**I. INTRODUCTION**

Understanding the size evolution of a nucleus with extreme numbers of protons and neutrons is a challenge for microscopic nuclear theory [1–7]. In recent years, simultaneous developments in experimental techniques, as well as atomic and nuclear theory, have provided great advances in our understanding of the nuclear size away from stability [8–11]. Accurate nuclear charge radii calculations with quantifiable uncertainties are now becoming available for light and medium mass nuclei, enabling detailed comparisons with experimental data [2,3,6,11,12]. Light nuclear systems with mass number $A < 40$, whose properties can now be assessed by different *ab initio* many-body methods [2,3,5,6,13,14], are a testing ground for nuclear theory. However, nuclear charge radii measurements of these systems are scarce, with most of the available data obtained from spectroscopic measurements of atomic isotope shifts (ISs) [11,12,15], whose uncertainties are dominated by calculated atomic parameters. The reason for this is that in light elements, spectroscopic changes from the nuclear size (field shifts, FSs) are much smaller than those related to the change in the nuclear mass (mass shifts, MSs), which are strongly affected by electron correlations [12]. Hence, the accuracy of atomic theory is one of the current main limitations for extending our knowledge of the nuclear size in this frontier region of the nuclear chart.

IS measurements cannot be compared directly with atomic calculations. Where at least three stable isotopes exist, independent charge radius measurements determined by muonic x-ray transition energies or elastic electron scattering [16] can

be used in combination with IS measurements to benchmark atomic calculations. However, this procedure cannot be applied to most odd-proton elements as they have only one stable isotope. The isotopes of Na ($Z = 11$) provide a distinct example of how joint developments in both atomic and nuclear theory are critical to guide our understanding of the evolution of the nuclear size. The IS measurements for these isotopes have existed since more than four decades [17]. However, it has been a major challenge to perform accurate atomic calculations required to extract the nuclear charge radii values from the experimental data. For this reason, Na isotopes are some of the rare cases where matter radii are known with higher precision than charge radii [18,19].

In this letter, we report on new accurate relativistic atomic calculations, with quantifiable uncertainties, that enable the extraction of charge radii for the Na isotopic chain. The available experimental data on matter radii combined with neutron skins calculated by *ab initio* nuclear theory are used to establish constraints on atomic parameters, providing guidance to the developments of atomic many-body theory.

II. ISOTOPE SHIFTS

Changes in the root-mean-squared nuclear charge radii, δr_c^2 , can be inferred from measurements of ISs, $\delta\nu$, using the linear expression [20]

$$\delta\nu^{A',A} = K(1/M_{A'} - 1/M_A) + F(\delta r_c^2)^{A',A}, \quad (1)$$

where K and F are the transition-dependent MS and FS constants, respectively, which are to a good approximation isotope-independent, and M_A is the nuclear mass for atomic number A . Corrections related to higher radial moments in the nuclear charge distribution are smaller than 0.5% [21], making them negligible as related to this work. The MS constant

*bohayon@ethz.ch

†bijaya@prl.res.in

is usually separated into $K = K_{\text{NMS}} + K_{\text{SMS}}$, with K_{NMS} and K_{SMS} the normal mass shift (NMS) and the specific mass shift (SMS) constants, respectively. For transitions in light systems, K_{NMS} can be estimated with a few per-mil precision by scaling the experimental excitation energy (E^{ex}) as $K_{\text{NMS}} = E^{\text{ex}} m_e$, where m_e is the electron mass [22–28]. However, accurate calculations of K_{SMS} are extremely challenging for systems with more than six electrons [14,29–34]. When given, the reported K_{SMS} uncertainties in many-electron systems are typically larger than 10% [11,12,35–39], thus limiting the accuracy of the extracted charge radii.

III. ATOMIC THEORY

We employ the relativistic coupled-cluster (RCC) theory, which is well suited for the accurate evaluation of correlations in many-electron atomic systems [40]. Traditionally, two procedures have been used to carry out these calculations: finite-field (FF) [23,41–43] and expectation-value-evaluation (EVE) [44,45]. These proved to have several limitations as detailed in Refs. [46,47]. The analytic response-based RCC (AR-RCC) theory was developed to circumvent these problems.

Recently, we have used the AR-RCC theory with singles and doubles approximation (AR-RCCSD) to estimate the IS constants for transitions in the indium atom [39,46], but calculations for Na and Mg^+ require further development by including higher-order electron correlations. Thus, we extend our AR-RCC theory to account for full triples excitations (AR-RCCSDT method). This method was recently benchmarked by performing extensive calculations on Li-like systems, for which more accurate methods are available. It was found to be more reliable than the FF and EVE approaches [47]. To validate the method for many-electron systems, we compare the calculated and measured values in Mg^+ , which has a similar electronic structure to Na. For Na, we develop a hybrid benchmarking method. It is based on comparing the neutron skin extracted in two ways. The first is from a combination of matter and charge radii, with the latter extracted using different values of K_{SMS} . The second is to calculate the skin directly using coupled-cluster (CC) many body nuclear theory as described next.

IV. NUCLEAR THEORY

Accurate *ab initio* calculations of charge radii are particularly challenging for open-shell nuclei. Shell-model calculations based on nonperturbative effective interactions derived from methods like valence-space in-medium similarity renormalization group [49–51] and shell-model based coupled-cluster [52], are complicated for nuclei where valence spaces consist of more than one major shell. Alternatively, methods based on single reference states that explicitly break symmetries may provide a conceptually simpler approach [5–7]. For charge radii, unprojected coupled-cluster theory carries small uncertainties from the lack of symmetry restoration [53], and in this work we follow Ref. [6] and employ single-reference CC theory. For alternative symmetry-projection techniques we refer the reader to Refs. [54–56].

For the CC calculations we employ the recently developed $\Delta\text{NNLO}_{\text{GO}}$ interaction [57] with a momentum cutoff of 450 MeV. These calculations are performed in the singles and doubles (CCSD) approximation [58–60] starting from an axially symmetric Hartree-Fock (HF) reference state. Parity, particle number, and the projection of total angular momentum onto the symmetry axis are conserved quantities. The HF calculations are performed in a harmonic-oscillator basis consisting of 15 major oscillator shells ($N_{\text{max}} = 14$), with a spacing of $\hbar\omega = 16$ MeV. The three-body interaction has an additional energy cut given by $E_{3\text{max}} = 16$, which is sufficiently large for the nuclei we compute. Once the HF solution is converged, a more accurate density matrix is computed using second-order many-body perturbation theory [61]. Diagonalization of this density matrix then yields the natural orbital basis [6,61,62]. Following Refs. [62,63], the normal-ordered Hamiltonian in the two-body approximation [64,65] is then truncated to a smaller model space ($N_{\text{max}}^{\text{nat}} = 12$) according to the occupation numbers of the natural orbits. The proton and neutron radii are calculated as ground-state expectation values. Charge radii include corrections from the Darwin-Foldy term and spin-orbit contributions as detailed in Refs. [66–69]. So far, we can only estimate the effects of symmetry restoration from projected HF calculations. The uncertainties of nuclear radii from model-space truncation, cluster truncations, and two different cutoffs for the $\Delta\text{NNLO}_{\text{GO}}$ interaction are estimated to be 2–3% following Refs. [6,11]. A full-fledged uncertainty analysis that also explores truncation effects from the chiral expansion and a variation of low-energy constants is beyond the scope of this work.

Odd-mass nuclei, such as the Na isotopes considered in this work, are more complicated than even-even nuclei because of the unpaired last nucleon. We performed quadrupole constrained HF calculations for a range of oblate and prolate deformations and found that in all cases (except for ^{25}Na) the prolate HF minimum provides the optimal reference state for the CC calculations. For ^{25}Na , starting from an oblate reference state yields the largest binding energy. The computation of odd-odd sodium isotopes are not performed in this work as accurate nuclear structure computations are challenged by two unpaired nucleons.

V. RESULTS AND DISCUSSION

In Table I we give the results for the ground-state properties of Na isotopes calculated by $\Delta\text{NNLO}_{\text{GO}}(450)$. Our uncertainty estimation is based on similar calculations in Ne, Mg, K, and Ca for the neutron skin [69] and radii [6,11]. The resulting calculated r_{np} are plotted in Fig. 1, and show a close to linear behavior within the uncertainty bounds.

Table II shows our results for the excitation energies (EEs) and IS constants of the $3S-3P_{1/2}$ (D1) and $3S-3P_{3/2}$ (D2) transitions in Na and Mg^+ at different levels of approximation in the atomic many-body method. The calculated energies are compared with the experimental values from Refs. [25,26] in the Supplemental Material [70]. Our final results for the EEs from the AR-RCCSDT method are in excellent agreement with the experimental values [25,26]. We find that by

TABLE I. Ground-state properties of the Na isotopic chain. Columns 2–5 give the charge, proton, neutron radii, and skin in fm, respectively, as calculated via Δ NNLO(450). Columns 6 and 7 give the experimental charge radii differences in fm², and absolute values in fm, respectively. Uncertainties (one standard deviation) from the IS measurements and nuclear calculation are given in parenthesis. Correlated uncertainties from the IS parameter calculation are in square brackets. Their behavior is portrayed in Fig. 3.

A	r_c^{Th}	r_p^{Th}	r_n^{Th}	r_{np}^{Th}	$(\delta r_c^2)^{23,A}$	r_c^{exp}
19	2.99(3)	2.87(3)	2.58(3)	−0.29(3)		
20					−0.60(9)[52]	2.89(2)[9]
21	3.03(3)	2.92(3)	2.82(3)	−0.09(3)	−0.13(5)[33]	2.97(1)[6]
22					−0.16(2)[16]	2.967(3)[27]
23	3.01(3)	2.90(3)	2.92(3)	0.02(3)		2.9935(38)
24					−0.02(4)[15]	2.990(7)[25]
25	2.97(3)	2.87(3)	2.98(3)	0.11(3)	0.12(5)[28]	3.013(8)[47]
26					0.34(2)[41]	3.049(4)[68]
27	3.01(3)	2.92(3)	3.11(3)	0.19(3)	0.60(5)[52]	3.091(8)[86]
28					0.89(7)[63]	3.14(1)[10]
29	3.03(3)	2.94(3)	3.25(3)	0.31(3)	1.4(1)[7]	3.22(1)[11]
30					1.7(2)[8]	3.26(2)[13]
31	3.06(3)	2.96(3)	3.33(3)	0.37(3)	2.2(1)[9]	3.34(1)[14]
33	3.13(3)	3.04(3)	3.49(3)	0.45(3)		

including triples excitations, the energy calculation accuracy is improved by an order of magnitude. The SMS constants are determined by considering relativistic form of the SMS operator as defined by [71]

$$O^{\text{SMS}} = \frac{1}{2} \sum_{i \neq j} \left[\vec{p}_i \cdot \vec{p}_j - \frac{\alpha Z}{r_i} \vec{\alpha}_i^D \cdot \vec{p}_j \right. \\ \left. - \frac{\alpha Z}{r_i} (\vec{\alpha}_i^D \cdot \vec{C}_i^1) (\vec{p}_j \cdot \vec{C}_j^1) \right], \quad (2)$$

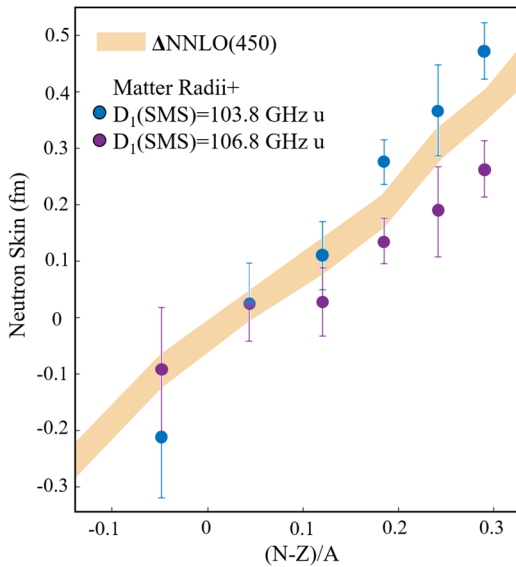


FIG. 1. Semiempirical estimation of K_{SMS} . We compare the calculated r_{np}^{Th} from Table I (filled band), with the semiempirical $r_{np}(K_{\text{SMS}})$ described in the main text.

TABLE II. Excitation energies (EE) (cm^{−1}) and IS constants F in (MHz/fm²), and K_{SMS} in (GHz u), for the D1 and D2 lines in Na and Mg⁺. Our calculations are given using the DHF and AR-RCCSD/T methods. Corrections from the Breit, QED and nuclear recoil effects are quoted as Δ Breit, Δ QED and Δ Recoil, respectively. The experimental F in Mg⁺ is taken from a King Plot [15]. The experimental K_{SMS} in Mg⁺ is derived from the results of Ref. [48] by subtracting the NMS and FS contributions.

EE	3S-3P _{1/2} (D1)		3S-3P _{3/2} (D2)	
	Na	Mg ⁺	Na	Mg ⁺
DHF	15921	34530	15937	34621
AR-RCCSD	16892	35634	16910	35732
AR-RCCSDT	16951(10)	35667(20)	16971(10)	35766(20)
Δ Breit	−0.44	0.55	−1.54	−4.85
Δ QED	−3.77	−8.91	−3.68	−8.65
Δ Recoil	−0.56	−1.40	−0.56	−1.40
Exp. [25,26]	16956.17	35669.31	16973.37	35760.88
F	Na	Mg ⁺	Na	Mg ⁺
DHF	−29.7	−104.5	−29.7	−104.6
AR-RCCSD	−38.9	−126.2	−38.9	−126.2
AR-RCCSDT	−39.3(3)	−126.4(7)	−39.2(3)	−126.4(7)
Δ Breit	0.0	0.1	0.0	0.1
Ref. [23]	−36.45	−123.2		
Ref. [41]	−39		−39	−127
Ref. [42]	−33	−127	−33	−127
Ref. [44]	−38.42	−125.81	−38.43	−125.82
Ref. [45]	−38.76	−126.22	−38.80	−126.32
Exp. [15]		−127(12)		
K_{SMS}	Na	Mg ⁺	Na	Mg ⁺
DHF	−106	37	−106	35
AR-RCCSD	131	403	131	403
AR-RCCSDT	109(3)	374(7)	109(3)	373(7)
Δ Breit	0.1	0.6	0.2	1.0
Semiemp.	105.3(1.3)			
Ref. [23]	98.5	406.1		
Ref. [41]	109(24)	379(12)	108(24)	373(6)
Ref. [42]	116	378	116	378
Ref. [43]		365		366
Ref. [44]	97	362	97	361
Ref. [45]	114.4	398.8	112.3	389.9
Exp. [48]		369.3(3)		367.7(3)

where α is the fine-structure constant, Z is the atomic number, and α^D is the Dirac operator. The differences between the AR-RCCSD and AR-RCCSDT values for F in all the states are found to be negligible. This finding is in line with our calculations for Li-like systems [47], where it was also found that both the EVE and AR methods produce reliable results for F , with only the FF method showing some spurious deviations. These two facts explain the agreement between our calculation and the previously reported FF [41,43] and EVE [44,45] results from the literature. The FF results of Refs. [23,42] show a more significant deviation. Our uncertainty for F is given by estimating the magnitude of neglected QED effects as detailed in Ref. [47], as well as neglecting higher order charge moments in the nuclear distribution.

In contrast to the results for calculations of F , we find triples excitations to be significant for the K_{SMS} constants in both systems, with their magnitude much larger than in Li-like systems [47]. This is indicated by the large change in K_{SMS} for both systems between the mean-field Dirac-Hartree-Fock (DHF) and the AR-RCCSD/T methods. This highlights the critical role of electron correlations in the determination of the above constant. On the other hand, higher-order relativistic effects, calculated using the Breit Hamiltonian, are found to be smaller than 0.3%, thus strengthening our assumption that K_{NMS} may be taken from the scaling-law with sufficient accuracy. The limited reliability of the FF and EVE approaches for estimating K_{SMS} [47,72], combined with the major role of triples excitations, account for the major spread in the previously calculated values. Only the values of Ref. [41], who utilized the FF approach in a nonrelativistic calculation, agrees with our calculations for both systems. However, their values for the individual levels differ considerably, as shown in the Supplemental Material [70].

Even though higher-order electron correlation effects, which can be captured by calculating quadruple excitations, do not contribute directly in the AR-RCC theory owing to the one-body and two-body forms of the FS and SMS operators, their inclusion can change the amplitudes of the unperturbed wave operators, causing an indirect modification to our results. An uncertainty of 2–3% was estimated by analyzing such contributions in a perturbative approach. For Na, this uncertainty is an order of magnitude smaller than that reported in the literature [41]. To validate the reliability of our calculated mass shifts, and their uncertainty, we carry out two benchmark tests: one from the atomic physics side and the other from the side of nuclear physics.

VI. BENCHMARK WITH Mg^+

We take advantage of the precise IS measurements in Mg^+ [48], and the reliability of our field shift calculation, to benchmark our method of obtaining the mass shift. First, the absolute radii $(r_c)^{24} = 3.0556(25)$, and $(r_c)^{26} = 3.0297(21)$ fm, are extracted from the Barrett-equivalent radii $(R_k^\alpha)^{24} = 3.9291(30)$, and $(R_k^\alpha)^{26} = 3.8992(27)$ fm measured with muonic x-rays [21], as well as the proportionality factors $(R_k^\alpha)^{24}/(r_c)^{24} = 1.2859(3)$ and $(R_k^\alpha)^{26}/(r_c)^{26} = 1.2870(2)$ which we extract from model-independent analysis of electron scattering experiments [73–75]. Accounting for correlations, we arrive at $(\delta r_c^2)_{24,26} = -0.158(9)$ fm, yielding an FS of 20.0(1.1) MHz. Employing Eq. (1) with this FS and with the NMS taken from the scaling law results in $K_{\text{SMS}} = 369.3(3)$ GHz u and $K_{\text{SMS}} = 367.7(3)$ GHz u for the D1 and D2 transitions, respectively. These values agree within one standard deviation with our calculated value of $K_{\text{SMS}} = 374(7)$ GHz u for both transitions. This test confirms the applicability of the scaling-law for ns - np transitions in light systems. In Na, relativistic effects are smaller than in Mg^+ while electron correlations are larger, so that the scaling-law is expected to be at least as applicable.

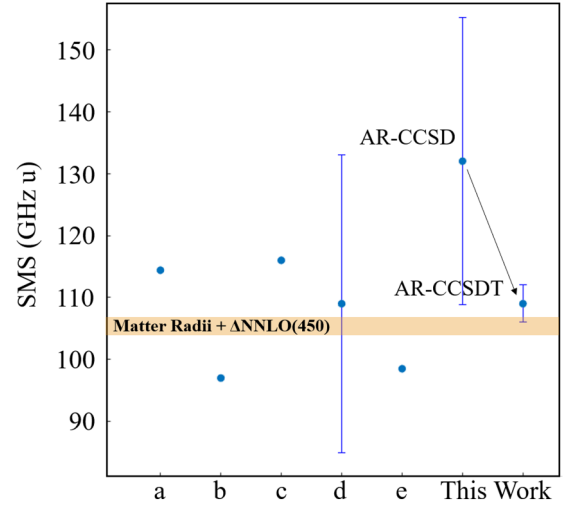


FIG. 2. Comparison of K_{SMS} in the $2S$ - $2p_{1/2}$ line of Na as calculated by (a) Ref. [45], (b) Ref. [44], (c) Ref. [42], (d) Ref. [41], (e) Ref. [23], and this work. The filled area is from the semiempirical estimation illustrated in Fig. 1.

VII. BENCHMARK WITH MATTER RADII AND NEUTRON SKIN

The neutron skin, defined as the difference between its proton and neutron radii, $r_{np} = r_n - r_p$, can be used to establish limits for the atomic parameters. This method has the benefit of incorporating information from measured matter radii r_m , thus limiting the role nuclear theory plays in this calculation. To do this we extract the experimental $r_c(K_{\text{SMS}})$ from the IS measurements as function of K_{SMS} , whilst keeping K_{NMS} and F constant as their uncertainty is negligible compared with that of K_{SMS} . Next, we calculate the point proton radius $r_p(K_{\text{SMS}})$ from $r_c(K_{\text{SMS}})$ by correcting it for nucleon RMS radii, the Darwin-Foldy term, and calculated spin orbit corrections [66–69]. The neutron radius $r_n(K_{\text{SMS}})$, from which $r_{np}(K_{\text{SMS}})$ is deduced, is then calculated from measured matter radii r_m [18,19] and $r_p(K_{\text{SMS}})$ through $r_m^2 = r_p^2 Z/A + r_n^2 N/A$ [66].

Figure 1 shows our semiempirical r_{np} estimation described above along with the directly calculated one from Table I. Scanning the value of K_{SMS} to fit the semiempirical skin and the theoretical one returns $K_{\text{SMS}} = 105.3(1.3)$ GHz u, which agrees with the direct calculation using AR-CCSDT of $K_{\text{SMS}} = 109(3)$ GHz u within their combined uncertainty. A comparison of the semiempirical K_{SMS} with ours and previous calculations is given in Fig. 2.

These two benchmarks validate the reliability of the central values and uncertainties calculated by the atomic theory, and serve as a striking test of the AR-CCSDT method and its applicability in light many-electron systems.

VIII. EXTRACTED CHARGE RADII

With the Na atomic constants calculated in this work (Table II), and the measured IS by Refs. [17,77–79], we deduce $(\delta r_c^2)^{23,A}$ directly from Eq. (1). The absolute radii are calculated using $(r_c)^{23} = 2.9935(38)$ fm. We deduce it

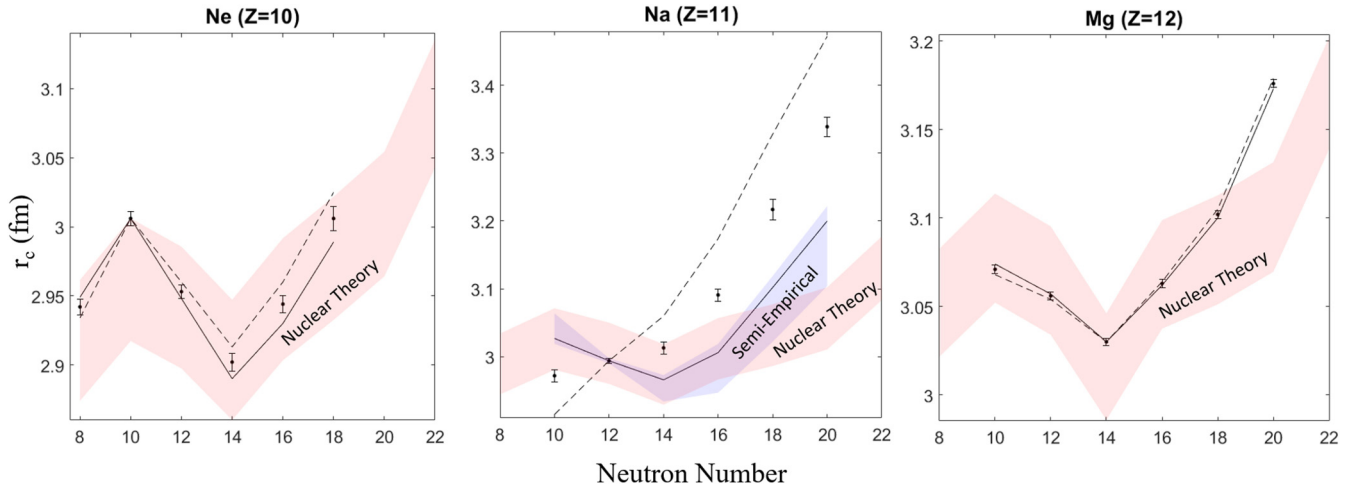


FIG. 3. Absolute charge radii of Ne, Na, and Mg. Experimental ISs are taken from Refs. [15,17,76–79]. The data-points give the central values with error bars from statistical uncertainty including that of the reference isotope. The full and broken lines give the spread resulting from the atomic parameters calculated in this work and in Ref. [80]. The filled bands represent the spread of values calculated by the nuclear theory. For Na, another band gives the values returned from the semiempirical neutron-skin fit of Fig. 1.

from the Barrett-equivalent radius $(R_k^\alpha)^{23} = 3.8492(31)$ fm [21], combined with a proportionality factor $(R_k^\alpha)^{23}/(r_c)^{23} = 1.286(1)$ estimated from electron scattering measurements on neighboring elements. Its uncertainty is given by the interpolation error. Our results are given in Table I, and shown in Fig. 3 along with predictions from nuclear theory. For completeness, we also include the charge radii of Ne [76,80] and Mg, with the latter extracted from IS measurements [15], and using our calculated F . Overall, nuclear theory predictions for r_c agree very well with experiment for both Ne and Mg, from $N = 10$ up to $N = 18$. This agreement suggests that the K_{SMS} value expected for Na isotopes sits at the lower edge of the confidence interval given by our atomic calculations. This conclusion is very much in line with the semiempirical prediction from the matter radii (neutron skins), as well as the difference between experimental and calculated K_{SMS} in Mg^+ . Further developments in atomic theory are needed to increase the precision in the calculated atomic parameters, e.g., by including a relativistic calculation of K_{NMS} , accounting for QED effects, and including quadruple excitations.

IX. SUMMARY AND OUTLOOK

Our ability to extract charge radii differences from spectroscopic measurements is limited by the difficulty in calculating many-body electron correlations. The resulting parameters often vary considerably between calculation methods and are missing a reliable uncertainty estimate. In this work, we developed the AR-RCC theory to include full triple

electron excitations and estimated quadrupole excitations perturbatively. This enabled us to extract for the first time model-independent charge radii for the Na isotopic chain, along with a realistic uncertainty estimate. To benchmark our calculation, we extended our work to Mg^+ , and found agreement with experimental values within our confidence intervals. This calculation also results in improved radii for the Mg isotopic chain. A further independent semiempirical benchmark is performed utilizing measured matter radii of Na combined with neutron skins calculated by state-of-the-art *ab initio* nuclear calculation. This work opens the gate to improved radii determinations for mono-isotopic elements across the nuclear table. A development timely with the progress of new radioactive beam facilities, such as FRIB, where exotic light nuclear systems will be produced up to the proton and neutron drip lines.

ACKNOWLEDGMENTS

The atomic physics calculations were carried out using the Vikram-100 HPC cluster of Physical Research Laboratory, Ahmedabad, India. This work is supported by Department of Energy, Office of Science, Office of Nuclear Physics, under Awards No. DE-SC0021176, No. DE-SC0021179, No. DE-FG02-96ER40963, and No. DE-SC0018223. Computer time was provided by the Innovative and Novel Computational Impact on Theory and Experiment (INCITE) programme. This research used resources of the Oak Ridge Leadership Computing Facility located at Oak Ridge National Laboratory, which is supported by the Office of Science of the Department of Energy under Contract No. DE-AC05-00OR22725.

[1] E. Caurier, K. Langanke, G. Martínez-Pinedo, F. Nowacki, and P. Vogel, Shell model description of isotope shifts in calcium, *Phys. Lett. B* **522**, 240 (2001).

[2] V. Lapoux, V. Somà, C. Barbieri, H. Hergert, J. D. Holt, and S. R. Stroberg, Radii and Binding Energies in Oxygen Isotopes: A Challenge for Nuclear Forces, *Phys. Rev. Lett.* **117**, 052501 (2016).

- [3] D. Lonardonì, J. Carlson, S. Gandolfi, J. E. Lynn, K. E. Schmidt, A. Schwenk, and X. B. Wang, Properties of Nuclei up to $A = 16$ Using Local Chiral Interactions, *Phys. Rev. Lett.* **120**, 122502 (2018).
- [4] A. Ekström, G. R. Jansen, K. A. Wendt, G. Hagen, T. Papenbrock, B. D. Carlsson, C. Forssén, M. Hjorth-Jensen, P. Navrátil, and W. Nazarewicz, Accurate nuclear radii and binding energies from a chiral interaction, *Phys. Rev. C* **91**, 051301(R) (2015).
- [5] V. Somà, P. Navrátil, F. Raimondi, C. Barbieri, and T. Duguet, Novel chiral Hamiltonian and observables in light and medium-mass nuclei, *Phys. Rev. C* **101**, 014318 (2020).
- [6] S. J. Novario, G. Hagen, G. R. Jansen, and T. Papenbrock, Charge radii of exotic neon and magnesium isotopes, *Phys. Rev. C* **102**, 051303(R) (2020).
- [7] V. Somà, C. Barbieri, T. Duguet, and P. Navrátil, Moving away from singly-magic nuclei with Gorkov Green's function theory, *Eur. Phys. J. A* **57**, 135 (2021).
- [8] A. J. Miller, K. Minamisono, A. Klose, D. Garand, C. Kujawa, J. D. Lantis, Y. Liu, B. Maaß, P. F. Mantica, W. Nazarewicz, W. Nörtershäuser, S. V. Pineda, P. G. Reinhard, D. M. Rossi, F. Sommer, C. Sumithrarachchi, A. Teigelhöfer, and J. Watkins, Proton superfluidity and charge radii in proton-rich calcium isotopes, *Nat. Phys.* **15**, 432 (2019).
- [9] R. F. Garcia Ruiz, M. L. Bissell, K. Blaum, A. Ekström, N. Frömmgen, G. Hagen, M. Hammen, K. Hebel, J. D. Holt, G. R. Jansen, M. Kowalska, K. Kreim, W. Nazarewicz, R. Neugart, G. Neyens, W. Nörtershäuser, T. Papenbrock, J. Papuga, A. Schwenk, J. Simonis *et al.*, Unexpectedly large charge radii of neutron-rich calcium isotopes, *Nat. Phys.* **12**, 594 (2016).
- [10] R. P. de Groote, J. Billowes, C. L. Binnersley, M. L. Bissell, T. E. Cocolios, T. Day Goodacre, G. J. Farooq-Smith, D. V. Fedorov, K. T. Flanagan, S. Franchoo, R. F. Garcia Ruiz, W. Gins, J. D. Holt, Á. Koszorús, K. M. Lynch, T. Miyagi, W. Nazarewicz, G. Neyens, P. G. Reinhard, S. Rothe *et al.*, Measurement and microscopic description of odd-even staggering of charge radii of exotic copper isotopes, *Nat. Phys.* **16**, 620 (2020).
- [11] Á. Koszorús, X. F. Yang, W. G. Jiang, S. J. Novario, S. W. Bai, J. Billowes, C. L. Binnersley, M. L. Bissell, T. E. Cocolios, B. S. Cooper, R. P. de Groote, A. Ekström, K. T. Flanagan, C. Forssén, S. Franchoo, R. F. Garcia Ruiz, F. P. Gustafsson, G. Hagen, G. R. Jansen, A. Kanellakopoulos *et al.*, Charge radii of exotic potassium isotopes challenge nuclear theory and the magic character of $N = 32$, *Nat. Phys.* **17**, 439 (2021).
- [12] H. Heylen, C. S. Devlin, W. Gins, M. L. Bissell, K. Blaum, B. Cheal, L. Filippin, R. F. Garcia Ruiz, M. Godefroid, C. Gorges, J. D. Holt, A. Kanellakopoulos, S. Kaufmann, Á. Koszorús, K. König, S. Malbrunot-Ettenauer, T. Miyagi, R. Neugart, G. Neyens, W. Nörtershäuser *et al.*, High-resolution laser spectroscopy of $^{27-32}\text{Al}$, *Phys. Rev. C* **103**, 014318 (2021).
- [13] Z. T. Lu, P. Mueller, G. W. F. Drake, W. Nörtershäuser, Steven C. Pieper, and Z. C. Yan, Colloquium: Laser probing of neutron-rich nuclei in light atoms, *Rev. Mod. Phys.* **85**, 1383 (2013).
- [14] B. Maaß, T. Hüther, K. König, J. Krämer, J. Krause, A. Lovato, P. Müller, K. Pachucki, M. Puchalski, R. Roth, R. Sánchez, F. Sommer, R. B. Wiringa, and W. Nörtershäuser, Nuclear Charge Radii of $^{10,11}\text{B}$, *Phys. Rev. Lett.* **122**, 182501 (2019).
- [15] D. T. Yordanov, M. L. Bissell, K. Blaum, M. De Rydt, Ch. Geppert, M. Kowalska, J. Krämer, K. Kreim, A. Krieger, P. Lievens, T. Neff, R. Neugart, G. Neyens, W. Nörtershäuser, R. Sánchez, and P. Vingerhoets, Nuclear Charge Radii of $^{21-32}\text{Mg}$, *Phys. Rev. Lett.* **108**, 042504 (2012).
- [16] G. Fricke, C. Bernhardt, K. Heilig, L. A. Schaller, L. Schellenberg, E. B. Shera, and C. W. DeJager, Nuclear ground-state charge radii from electromagnetic interactions, *At. Data Nucl. Data Tables* **60**, 177 (1995).
- [17] G. Huber, F. Touchard, S. Büttgenbach, C. Thibault, R. Klapisch, H. T. Duong, S. Liberman, J. Pinard, J. L. Vialle, P. Juncar, and P. Jacquinet, Spins, magnetic moments, and isotope shifts of $^{21-31}\text{Na}$ by high resolution laser spectroscopy of the atomic D_1 line, *Phys. Rev. C* **18**, 2342 (1978).
- [18] T. Suzuki, H. Geissel, O. Bochkarev, L. Chulkov, M. Golovkov, N. Fukunishi, D. Hirata, H. Irnich, Z. Janas, H. Keller, T. Kobayashi, G. Kraus, G. Münzenberg, S. Neumaier, F. Nickel, A. Ozawa, A. Piechaczek, E. Roeckl, W. Schwab, K. Sümmerer *et al.*, Nuclear radii of Na and Mg isotopes, *Nucl. Phys. A* **630**, 661 (1998).
- [19] S. Suzuki, M. Takechi, T. Ohtsubo, D. Nishimura, M. Fukuda, T. Kuboki, M. Nagashima, T. Suzuki, T. Yamaguchi, A. Ozawa, H. Ohishi, T. Moriguchi, T. Sumikama, H. Geissel, N. Aoi, Rui-Jiu Chen, De-Qing Fang, N. Fukuda, S. Fukuoka, H. Furuki *et al.*, Measurements of interaction cross sections for $^{22-35}\text{Na}$ isotopes, in *European Physical Journal Web of Conferences*, Vol. 66 (EDP Sciences, Les Ulis, France, 2014), p. 03084.
- [20] W. H. King, *Isotope Shifts in Atomic Spectra* (Springer Science & Business Media, Berlin, 2013).
- [21] G. Fricke and K. Heilig, *Nuclear Charge Radii*, edited by H. Schopper (Springer-Verlag, Berlin, 2004).
- [22] H. A. Bethe and E. E. Salpeter, *Quantum Mechanics of One- and Two-Electron Atoms* (Springer US, New York, NY, 1977).
- [23] I. I. Tupitsyn, V. M. Shabaev, J. R. Crespo López-Urrutia, I. Draganić, R.S. Orts, and J. Ullrich, Relativistic calculations of isotope shifts in highly charged ions, *Phys. Rev. A* **68**, 022511 (2003).
- [24] M. G. Kozlov and V. A. Korol, Relativistic and correlation corrections to isotope shift in Ba II and Ba I (unpublished, 2007).
- [25] J. F. Baugh, C. E. Burkhardt, J. J. Leventhal, and T. Bergeman, Precision Stark spectroscopy of sodium ^2P and ^2D states, *Phys. Rev. A* **58**, 1585 (1998).
- [26] V. Kaufman and W. C. Martin, Wavelengths and energy level classifications of magnesium spectra for all stages of ionization (Mg I through Mg XII), *J. Phys. Chem. Ref. Data* **20**, 83 (1991).
- [27] J. G. Li, C. Nazé, M. Godefroid, G. Gaigalas, and P. Jönsson, On the breakdown of the dirac kinetic energy operator for estimating normal mass shifts, *Eur. Phys. J. D* **66**, 290 (2012).
- [28] Y. S. Kozhedub, A. V. Volotka, A. N. Artemyev, D. A. Glazov, G. Plunien, V. M. Shabaev, I. I. Tupitsyn, and Th. Stöhlker, Relativistic recoil, electron-correlation, and QED effects on the $2p_j-2s$ transition energies in Li-like ions, *Phys. Rev. A* **81**, 042513 (2010).
- [29] S. Bubin, M. Pavanello, W. C. Tung, Keeper L. Sharkey, and L. Adamowicz, Born–Oppenheimer and non-Born–Oppenheimer, atomic and molecular calculations with explicitly correlated Gaussians, *Chem. Rev.* **113**, 36 (2013).
- [30] M. Puchalski, J. Komasa, and K. Pachucki, Explicitly correlated wave function for a boron atom, *Phys. Rev. A* **92**, 062501 (2015).

- [31] N. A. Zubova, A. V. Malyshev, I. I. Tupitsyn, V. M. Shabaev, Y. S. Kozhedub, G. Plunien, C. Brandau, and Th. Stöhlker, Isotope shifts of the $2p_{3/2}$ - $2p_{1/2}$ transition in B-like ions, *Phys. Rev. A* **93**, 052502 (2016).
- [32] V. A. Yerokhin, R. A. Müller, A. Surzhykov, P. Micke, and P. O. Schmidt, Nonlinear isotope-shift effects in Be-like, B-like, and C-like argon, *Phys. Rev. A* **101**, 012502 (2020).
- [33] I. Hornyák, L. Adamowicz, and S. Bubin, Low-lying 2S states of the singly charged carbon ion, *Phys. Rev. A* **102**, 062825 (2020).
- [34] M. Puchalski, J. Komasa, and K. Pachucki, Fine and hyperfine splitting of the low-lying states of ^9Be , *Phys. Rev. A* **104**, 022824 (2021).
- [35] B. Cheal, T. E. Cocolios, and S. Fritzsche, Laser spectroscopy of radioactive isotopes: Role and limitations of accurate isotope-shift calculations, *Phys. Rev. A* **86**, 042501 (2012).
- [36] R. Ferrer, N. Bree, T.E. Cocolios, I.G. Darby, H. De Witte, W. Dexters, J. Diriken, J. Elseviers, S. Franchoo, M. Huysse, N. Kesteloot, Yu. Kudryavtsev, D. Pauwels, D. Radulov, T. Roger, H. Savajols, P. Van Duppen, and M. Venhart, In-gas-cell laser ionization spectroscopy in the vicinity of ^{100}Sn : Magnetic moments and mean-square charge radii of $N=50$ – 54 Ag, *Phys. Lett. B* **728**, 191 (2014).
- [37] H. Heylen, C. Babcock, R. Beerwerth, J. Billowes, M. L. Bissell, K. Blaum, J. Bonnard, P. Campbell, B. Cheal, T. Day Goodacre, D. Fedorov, S. Fritzsche, R. F. Garcia Ruiz, W. Geithner, Ch. Geppert, W. Gins, L. K. Grob, M. Kowalska, K. Kreim, S. M. Lenzi *et al.*, Changes in nuclear structure along the Mn isotopic chain studied via charge radii, *Phys. Rev. C* **94**, 054321 (2016).
- [38] Z. Zuhrianda, High precision calculation for the development of atomic clock and the search beyond the standard model, Ph.D. thesis, 2017.
- [39] B. K. Sahoo, A. R. Vernon, R. F. Garcia Ruiz, C. L. Binnersley, J. Billowes, M. L. Bissell, T. E. Cocolios, G. J. Farooq-Smith, K. T. Flanagan, W. Gins, R. P. de Groote, Á. Koszorús, G. Neyens, K. M. Lynch, F. Parnefjord-Gustafsson, C. M. Ricketts, K. D. A. Wendt, S. G. Wilkins, and X. F. Yang, Analytic response relativistic coupled-cluster theory: The first application to indium isotope shifts, *New J. Phys.* **22**, 012001 (2020).
- [40] I. Lindgren and J. Morrison, Atomic many-body theory, *Springer Ser. Chem. Phys.* (1982).
- [41] J. C. Berengut, V. A. Dzuba, and V. V. Flambaum, Isotope-shift calculations for atoms with one valence electron, *Phys. Rev. A* **68**, 022502 (2003).
- [42] V. A. Korol and M. G. Kozlov, Relativistic corrections to the isotope shift in light ions, *Phys. Rev. A* **76**, 022103 (2007).
- [43] S. Roy and S. Majumder, *Ab initio* estimations of the isotope shift for the first three elements of the K isoelectronic sequence, *Phys. Rev. A* **92**, 012508 (2015).
- [44] M. S. Safronova and W. R. Johnson, Third-order isotope-shift constants for alkali-metal atoms and ions, *Phys. Rev. A* **64**, 052501 (2001).
- [45] B. K. Sahoo, Accurate estimate of α variation and isotope shift parameters in Na and Mg^+ , *J. Phys. B: At., Mol. Opt. Phys.* **43**, 231001 (2010).
- [46] A. R. Vernon, C. M. Ricketts, J. Billowes, T. E. Cocolios, B. S. Cooper, K. T. Flanagan, R. F. Garcia Ruiz, F. P. Gustafsson, G. Neyens, H. A. Perrett *et al.*, Laser spectroscopy of indium rydberg atom bunches by electric field ionization, *Sci. Rep.* **10**, 1 (2020).
- [47] B. K. Sahoo and B. Ohayon, Benchmarking many-body approaches for the determination of isotope-shift constants: Application to the Li, Be^+ , and Ar^{15+} isoelectronic systems, *Phys. Rev. A* **103**, 052802 (2021).
- [48] V. Batteiger, S. Knünz, M. Herrmann, G. Saathoff, H. A. Schüssler, B. Bernhardt, T. Wilken, R. Holzwarth, T. W. Hänsch, and Th. Udem, Precision spectroscopy of the $3s$ - $3p$ fine-structure doublet in Mg^+ , *Phys. Rev. A* **80**, 022503 (2009).
- [49] H. Hergert, S. K. Bogner, T. D. Morris, A. Schwenk, and K. Tsukiyama, The In-Medium Similarity Renormalization Group: A novel *ab initio* method for nuclei, *Phys. Rep.* **621**, 165 (2016).
- [50] S. R. Stroberg, A. Calci, H. Hergert, J. D. Holt, S. K. Bogner, R. Roth, and A. Schwenk, Nucleus-Dependent Valence-Space Approach to Nuclear Structure, *Phys. Rev. Lett.* **118**, 032502 (2017).
- [51] T. Miyagi, S. R. Stroberg, J. D. Holt, and N. Shimizu, *Ab initio* multishell valence-space Hamiltonians and the island of inversion, *Phys. Rev. C* **102**, 034320 (2020).
- [52] Z. H. Sun, T. D. Morris, G. Hagen, G. R. Jansen, and T. Papenbrock, Shell-model coupled-cluster method for open-shell nuclei, *Phys. Rev. C* **98**, 054320 (2018).
- [53] G. Hagen, S. J. Novario, Z. H. Sun, T. Papenbrock, G. R. Jansen, J. G. Lietz, T. Duguet, and A. Tichai, Angular-momentum projection in coupled-cluster theory: Structure of ^{34}Mg , [arXiv:2201.07298](https://arxiv.org/abs/2201.07298).
- [54] Mikael Frosini, Thomas Duguet, Jean-Paul Ebran, and Vittorio Somà, Multi-reference many-body perturbation theory for nuclei I—Novel PGCM-PT formalism, [arXiv:2110.15737](https://arxiv.org/abs/2110.15737).
- [55] Mikael Frosini, Thomas Duguet, Jean-Paul Ebran, Benjamin Bally, Tobias Mongelli, Tomás R. Rodríguez, Robert Roth, and Vittorio Somà, Multi-reference many-body perturbation theory for nuclei. II. *Ab initio* study of neon isotopes via PGCM and IM-NCSM calculations, [arXiv:2111.00797](https://arxiv.org/abs/2111.00797).
- [56] Mikael Frosini, Thomas Duguet, Jean-Paul Ebran, Benjamin Bally, Heiko Hergert, Tomás R. Rodríguez, Robert Roth, Jiangming Yao, and Vittorio Somà, Multi-reference many-body perturbation theory for nuclei III—*Ab initio* calculations at second order in PGCM-PT, [arXiv:2111.01461](https://arxiv.org/abs/2111.01461).
- [57] W. G. Jiang, A. Ekström, C. Forssén, G. Hagen, G. R. Jansen, and T. Papenbrock, Accurate bulk properties of nuclei from $A = 2$ to ∞ from potentials with Δ isobars, *Phys. Rev. C* **102**, 054301 (2020).
- [58] H. Kümmel, K. H. Lührmann, and J. G. Zabolitzky, Many-fermion theory in expS- (or coupled cluster) form, *Phys. Rep.* **36**, 1 (1978).
- [59] R. J. Bartlett and M. Musiał, Coupled-cluster theory in quantum chemistry, *Rev. Mod. Phys.* **79**, 291 (2007).
- [60] G. Hagen, T. Papenbrock, M. Hjorth-Jensen, and D. J. Dean, Coupled-cluster computations of atomic nuclei, *Rep. Prog. Phys.* **77**, 096302 (2014).
- [61] A. Tichai, J. Müller, K. Vobig, and R. Roth, Natural orbitals for *ab initio* no-core shell model calculations, *Phys. Rev. C* **99**, 034321 (2019).
- [62] J. Hoppe, A. Tichai, M. Heinz, K. Hebeler, and A. Schwenk, Natural orbitals for many-body expansion methods, *Phys. Rev. C* **103**, 014321 (2021).
- [63] M. Heinz, A. Tichai, J. Hoppe, K. Hebeler, and A. Schwenk, In-medium similarity renormalization group with three-body operators, *Phys. Rev. C* **103**, 044318 (2021).

- [64] G. Hagen, T. Papenbrock, D. J. Dean, A. Schwenk, A. Nogga, M. Włoch, and P. Piecuch, Coupled-cluster theory for three-body Hamiltonians, *Phys. Rev. C* **76**, 034302 (2007).
- [65] R. Roth, S. Binder, K. Vobig, A. Calci, J. Langhammer, and P. Navrátil, Medium-Mass Nuclei with Normal-Ordered Chiral $NN+3N$ Interactions, *Phys. Rev. Lett.* **109**, 052501 (2012).
- [66] G. P. Kamuntavičius, Root-mean-square radii of light atomic nuclei: Neutron skin, *Phys. Rev. C* **56**, 191 (1997).
- [67] J. L. Friar, J. Martorell, and D. W. L. Sprung, Nuclear sizes and the isotope shift, *Phys. Rev. A* **56**, 4579 (1997).
- [68] T. Yamaguchi, I. Hachiuma, A. Kitagawa, K. Namihira, S. Sato, T. Suzuki, I. Tanihata, and M. Fukuda, Scaling of Charge-Changing Interaction Cross Sections and Point-Proton Radii of Neutron-Rich Carbon Isotopes, *Phys. Rev. Lett.* **107**, 032502 (2011).
- [69] G. Hagen, A. Ekström, C. Forssén, G. R. Jansen, W. Nazarewicz, T. Papenbrock, K. A. Wendt, S. Bacca, N. Barnea, B. Carlsson, C. Drischler, K. Hebeler, M. Hjorth-Jensen, M. Miorelli, G. Orlandini, A. Schwenk, and J. Simonis, Neutron and weak-charge distributions of the ^{48}Ca nucleus, *Nat. Phys.* **12**, 186 (2016).
- [70] See Supplemental Material at <http://link.aps.org/supplemental/10.1103/PhysRevC.105.L031305> for the calculated energies and IS constants for the individual levels, as well our recommended charge radii for the Mg chain.
- [71] C. W. P. Palmer, Reformulation of the theory of the mass shift, *J. Phys. B* **20**, 5987 (1987).
- [72] A. Dorne, B. K. Sahoo, and A. Kastberg, Relativistic coupled-cluster calculations of isotope shifts for the low-lying states of Ca II in the finite-field approach, *Atoms* **9**, 26 (2021).
- [73] G. C. Li, M. R. Yearian, and I. Sick, High-momentum-transfer electron scattering from ^{24}Mg , ^{27}Al , ^{28}Si , and ^{32}S , *Phys. Rev. C* **9**, 1861 (1974).
- [74] R. Soundranayagam, A. Saha, Kamal K. Seth, C.W. de Jager, H. de Vries, H. Blok, and G. van der Steenhoven, Ground-state charge distribution of ^{26}Mg , *Phys. Lett. B* **212**, 13 (1988).
- [75] H. De Vries, C.W. De Jager, and C. De Vries, Nuclear charge-density-distribution parameters from elastic electron scattering, *At. Data Nucl. Data Tables* **36**, 495 (1987).
- [76] K. Marinova, W. Geithner, M. Kowalska, K. Blaum, S. Kappertz, M. Keim, S. Kloos, G. Kotrotsios, P. Lievens, R. Neugart, H. Simon, and S. Wilbert, Charge radii of neon isotopes across the sd neutron shell, *Phys. Rev. C* **84**, 034313 (2011).
- [77] G. Huber, C. Thibault, R. Klapisch, H. T. Duong, J. L. Vialle, J. Pinard, P. Juncar, and P. Jacquinet, High-Resolution Laser Spectroscopy of the d Lines of On-Line Produced $^{21,22,24,25}\text{Na}$ Using a New High-Sensitivity Method of Detection of Optical Resonances, *Phys. Rev. Lett.* **34**, 1209 (1975).
- [78] K. Pescht, H. Gerhardt, and E. Matthias, Isotope shift and HFS of D1 lines in Na-22 and 23 measured by saturation spectroscopy, *Z. Phys. A: At. Nucl.* **281**, 199 (1977).
- [79] F. Touchard, J. M. Serre, S. Büttgenbach, P. Guimbal, R. Klapisch, M. de Saint Simon, C. Thibault, H. T. Duong, P. Juncar, S. Liberman, J. Pinard, and J. L. Vialle, Electric quadrupole moments and isotope shifts of radioactive sodium isotopes, *Phys. Rev. C* **25**, 2756 (1982).
- [80] B. Ohayon, H. Rahangdale, A. J. Geddes, J. C. Berengut, and G. Ron, Isotope shifts in $^{20,22}\text{Ne}$: Precision measurements and global analysis in the framework of intermediate coupling, *Phys. Rev. A* **99**, 042503 (2019).